## Supplementary Material A: Literature overview of studies on global hydrological effects of climate change

| *Study* | *Climate model* | *Scenario* | *Runoff* | *Method* | *Horizon* | *Parameters* | *Significance / Consistency* | *Rivers / Regions* | *Results* |
|---|---|---|---|---|---|---|---|---|---|
| Aerts (2006) | ECBilt-CLIO-VECODE | A2 | Hydrological model: STREAM including simplified routing scheme | Direct use of GCM meteo data | 21[st] century | - Mean decadal change in discharge compared to discharge 1750-2000<br>- Inter decadal variability compared with natural variability | ~<br>Comparison to past variability | Globe<br>Amazon, Congo,Danube, Ganges, Lena,Mekong Mississipi, Murray, Nile, Odra, Rhine, Syr-Darya, Yukon, Volga,Volta | Discharge increase: Congo, Mekong, Ganges, Amazon, Rhine, Murray, Volga<br>Discharge decrease: Nile, Danube, Mississippi<br>Seasonal shift: Lena |
| Alcamo (2002) | ECHAM4<br>HadCM3 | A2, B2 | Hydrological model: WaterGAP including routing | Change factor | 2020s, 2050s, 2080s | - Annual withdrawal-to-availability ratio<br>- Consumption- to-Q90 ratio<br>- Per capita wa-ter availability | Overlap between three parameters selected as indicators of climate change | Globe | Severe water stress: Southwester USA, central Mexico, northeast Brazil, West Coast Latin America, northern and southern Africa, Middle East |
| Arnell (1999b) | HadCM2<br>HadCM3 | 1% per year CO2 increase | Hydrological model, no routing | Change factor | 2020s, 2050s, 2080s | - Average annual runoff<br>- Water Stress | - | Globe<br>42 rivers | Change in high flow: North-America, east Asia, Ghana<br>Increasing water stress: Mediterranean region, Middle-East, South- Africa, parts of south Asia<br>Seasonal shift: Belarus |
| Arnell (2003, 2004) | HadCM3<br>CGCM2<br>CSIRO Mk2<br>ECHAM4<br>GFDL_R30_c<br>CCSR/NIES2 | A1, A2, B1, B2 | Hydrological model, routing with monthly output | Change factor | 2020s, 2050s, 2080s | Average annual runoff<br>Drought runoff<br>InterAnnual variability<br>Flood runoff<br>Annual cycle | Consistency among scenarios, compared to consistency among models | Globe | Runoff increase: High latitudes, east Africa, south and east Asia<br>Runoff decrease: Southern and eastern Europe, western Russia, Middle East, Africa and much of North- and South-Africa |
| Arora and Boer (2001) | CGCM1 | GHG+A based on IS92a | runoff from from GCM as input for routing model | Direct use of GCM runoff fields | 2070-2100 | Mean discharge, amplitude and phase, flood discharge, annual max discharge and sdv, flow duration curve | - | Globe<br>23 rivers | Runoff decrease: Africa, Amazon, Yangtze, Mekong. Global decrease 14%<br>Seasonal shift, decrease in amplitude: Mid- and High latitude rivers |

| *Study* | *Climate model* | *Scenario* | *Runoff* | *Method* | *Horizon* | *Parameters* | *Significance / Consistency* | *Rivers / Regions* | *Results* |
|---|---|---|---|---|---|---|---|---|---|
| Manabe (2004) | GFDL-GCM ensemble of 8 experiments | IS92a, CO2 quadrup-ling | Discharge derived from runoff fields GCMs | Direct use of GCM runoff fields | 2050 | Change in annual mean runoff<br>Spatial pattern of change in seasonal soil moisture | - | Globe<br>42 rivers | Discharge increase: globally 7.3% by 2050, Arctic rivers, Brazil, Andes, northern India, Tibet, Indonesia, West-Africa, Amazon, Ganges, Brahmaputra<br>Discharge decrease: Nile, Mekong<br>Soil moisture decrease: North-America, Mediterranean Coast, northeast China, grasslands of Africa and southern and western regions of Australia |
| Milly (2005) | 12 GCMs (best models from ensemble of 21 IPCC AR4 models) | A1B | Runoff fields from GCMs as input for routing model | Direct use of GCM runoff fields | 2041-2060 | Annual mean change compared with past trends | Number of models showing positive changes minus number of models showing negative change | Globe | Runoff decrease: Southern Europe, Middle-East, mid-latitude western North-America, southern Africa<br>Runoff increase: High latitude North-America, Eurasia, South-America, eastern equatorial Africa |
| Nohara (2006) | ensemble of 19 AOGCMs (part of IPCC AR4) | A1B | runoff fields from GCM as input for routing model | Direct use of GCM runoff fields | 2100 | Mean annual change in runoff<br>River regimes | - Ensemble change relative to intermodel variability of the change signal<br>- GCM deviations for control run | Globe, 24 major rivers | Discharge increase: Northern Hemisphere (Arctic rivers), southern to eastern Asia (Mekong, Ganges), central Africa<br>Discharge decrease: Central America, southern Africa, Mediterranean region, southern North-America, Rhine, Danube<br>Seasonal shift: Arctic and mid-latitude rivers |

| Study | Climate model | Scenario | Runoff | Method | Horizon | Parameters | Significance / Consistency | Rivers / Regions | Results |
|---|---|---|---|---|---|---|---|---|---|
| Nijssen (2001) | HCCPR-CM2, HCCPR-MC3, ECHAM4, DOE-PCM3 (selected on resolution out of eight GCMs) | IS92a, A,B,C | Hydrological model: VIC including routing | Basin wide change factor | 2025<br>2045 | Annual hydrological cycle<br>Change in water balance<br>Seasonal change<br>Moisture deficit periods<br>Basin sensitivity | - | Amazon, Amur, MacKenzie, Xi, Mekong, Yellow River, Yenisei, Mississippi, Severnaya Dvina | Discharge increase: Arctic rivers<br>Discharge decrease: mid-latitude and tropic basins<br>Seasonal shift: Arctic rivers |
| Vörösmarty (2000) | HadCM2, CGCM1 | | Hydrological model: WBM including routing | Direct use of GCM meteo ata<br>Change factor for discharge change | 2025 | Water stress<br>Annual runoff | - | Globe | Decreased water availability: East Africa, southeast Asia, Mexico, Spain, parts of North- and South-America |
| This study | BCM2.0, CGCM3.1, CGCM2.3.2, CSIRO-Mk3.0, ECHAM5, ECHO-G, GFDL-CM2.1, GISS_ER, HADGEM1, IPSL-CM4, MIROC3.2medres, NCAR-CCSM3 | A1B and A2 | Hydrological model: PCRGLOB-WB including routing | Direct use of meteo data | 2100 | Mean, max and minimum annual runoff, annual cycle, inter-annual variability | - Significance compared to natural variability and ensemble uncertainty<br>- Consistency amongst GCMs | Globe, 20 major rivers | Discharge increase: Arctic rivers<br>Discharge decrease: Southern Australia, southern Africa, Mediterranean region, southwest South-America<br>Seasonal shift: Sub-Arctic rivers |

## Supplementary Material B: Penman-Monteith vs Blaney-Criddle

For most GCMs reference potential evaporation is calculated with a modification of the Penman-Monteith equation (Allen et al., 1998; Van Beek, 2008; Sperna Weiland at al., 2010). However, for some GCMs several input variables (e.g. wind speed, air pressure, radiation) required to calculate the Penman-Monteith evaporation were missing. For these GCMs the Blaney-Criddle equation is used (Brouwer and Heibloem, 1986; Oudin et al., 2005). The Blaney-Criddle equation is a simple temperature based potential evaporation estimator, whereas Penman-Monteith considers aerodynamics and radiation as well.

For several GCMs we compared potential evaporation calculated with the Penman-Monteith and the Blaney-Criddle equations and their resulting discharges. For brevity results are only shown for the CGCM2.3.2 model (Fig. 11a and b). For most GCMs potential evaporation calculated with the Penman-Monteith equation is high compared to Blaney-Criddle potential evaporation in Northern Australia, the Sahara, Southern Africa, the southwest US and Northern India and relatively low for Europe, the northen US, Canada, Russia, southeast Asia and the Amazon. However, only for specific periods, and in regions where evaporation limitation by soil moisture conditions is small, deviations in potential evaporation will introduce deviations in actual evaporation and runoff. Fig. 11c shows the percentage difference in discharge calculated using either the Blaney-Criddle or the Penman-Monteith potential evaporation. Deviations are large for the northern regions of the northern Hemisphere, the Amazon basin, Europe and parts of southeast Asia where discharge calculated with Penman-Monteith potential evaporation is relatively high. The Penman-Monteith based discharge is relatively low in arid regions, the Indus basin and Himalayas. Unfortunately hydrological studies are restricted to the available GCM datasets and, since not all required Penman-Monteith variables are reported for all GCMs, the use of a simple temperature based equation like Blaney-Criddle can not be avoided. Still, for those GCMs where all variables were available we preferred to use the FAO recommended Penman-Monteith equation (Allen et al., 1998).

In this study not the absolute discharge quantities, but the changes in average discharge and discharge extremes were of interest. Therefore we analyzed the influence of using either Blaney-Criddle or Penman-Monteith potential evaporation as input to the hydrological model on the resulting discharge changes. Hereto discharge changes derived with the hydrological model forced with Blaney-Criddle potential evaporation are regressed on discharge changes derived with the hydrological model forced with Penman-Monteith potential evaporation (Fig. 12). For this analysis we used data from the first realization of CGCM2.3.2 for the 20C3M experiment and A1B scenario. Overall, for 2100, the different potential evaporation equations result in similar directions of change. There are two exceptions. The first is the direction of change for maximum discharge in the MacKenzie, which is negative when using the Blaney-Criddle equation and positive for the Penman-Monteith equation. This is a result of the large differences in absolute discharge quantities for the MacKenzie which tend to be twice as high for the Penman-Monteith equation. The second exception is the Ganges where minimum discharge decreases with the Penman-Monteith method, while it increases for the Blaney-Criddle method. For the remaining catchments directions of change in minimum, maximum and mean discharge are the same when using either two equations. In general the projected changes follow the 1:1 slope, although differences in magnitude of projected change exist.

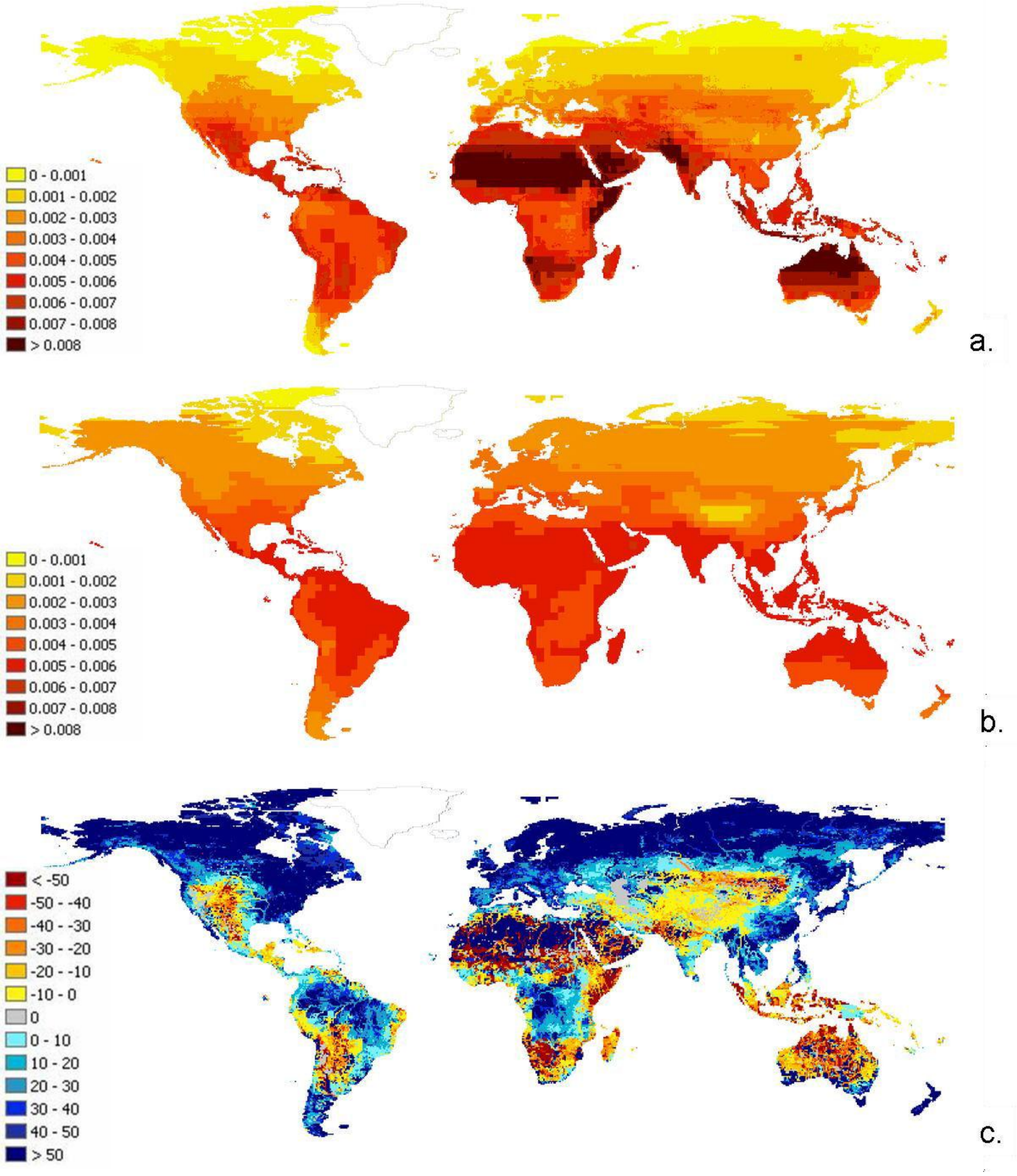


Figure 11: Maps with reference potential evaporation (m/day) and resulting percentage discharge difference (%). Fig. 11a. twenty year average reference potential evaporation (m/day) calculated with the Penman-Monteith equation. Fig. 11b. twenty year average reference potential evaporation (m/day) calculated with the Blaney-Criddle equation and Fig. 11c. percentage difference (%) between twenty year average discharges calculated with PCR-GLOBWB from either Penman-Monteith or Blaney-Criddle.

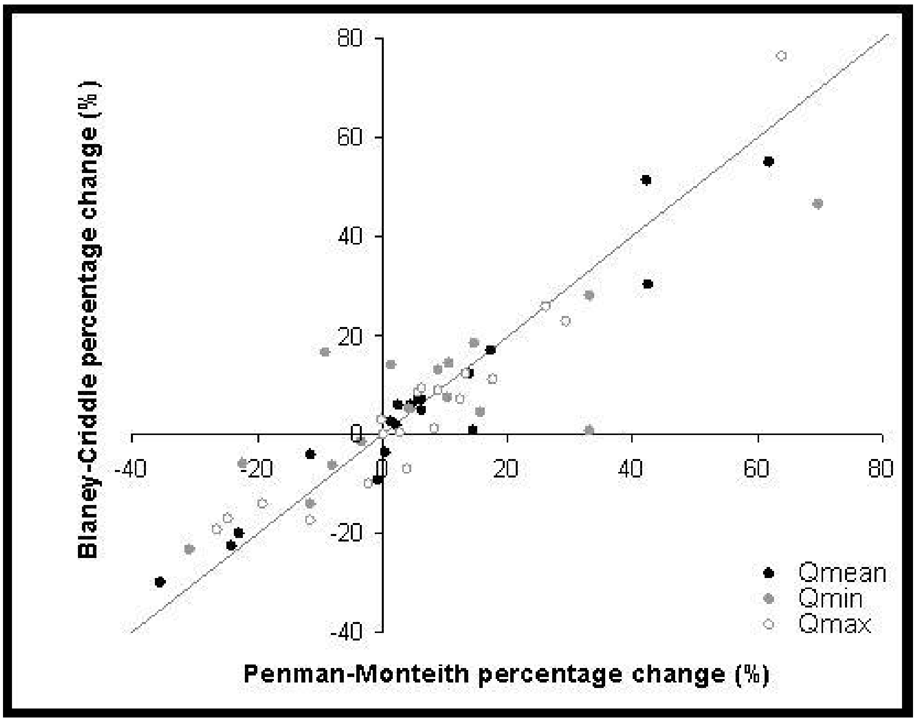


Figure 12: Percentage change in discharge calculated using potential evaporation derived with Blaney-Criddle vs Penman-Monteith. Black dots represent projected change in average discharge, grey dot represent changes in high flows (Qmax), white dots represent changes in low flows (Qmin). The solid line represents the 1:1 slope.

## Supplementary Material C: Consistency of change for multiple realizations of one GCM

For CGCM2.3.2, the GCM with the highest number of realizations for both the 20C3M experiment and the A1B scenario, we calculated change in discharge by 2100 for all five available realizations. Boxplots of projected changes for the 19 catchments are shown in Fig. 13a. Fig. 13b shows boxplots of changes projected by the twelve individual GCMs included in our ensemble. The boxplots of the five realizations of CGCM2.3.2 cover much smaller ranges than the boxplots derived from the ensemble of GCMs. Furthermore, for 13 out of 19 catchments the direction of change is consistent for all five realizations of the CGCM2.3.2 model. In Fig. 14a a global map with the number of CGCM2.3.2 realizations projecting change in the dominant direction (the direction of change projected by the majority of GCMs) is shown. For 55% of the globe all five realizations agree on the projected direction of change, for 81% of the globe at least four realizations agree on the direction of change and for the remaining 19% only three realizations are consistent.

From these results two conclusions can be drawn. Firstly, Fig. 13 shows the inter-model uncertainty is much larger than the intra-model uncertainty, at least for the GCM data we have at our disposal. And secondly, for the majority of catchments the projected directions of change are consistent for the five realizations. This indicates that including different numbers of realizations for the individual GCMs in our ensemble would result in overweighting the direction of change projected by the GCMs with multiple realizations. Therefore we restricted ourselves to a single realization for each of the twelve GCMs included in the ensemble.

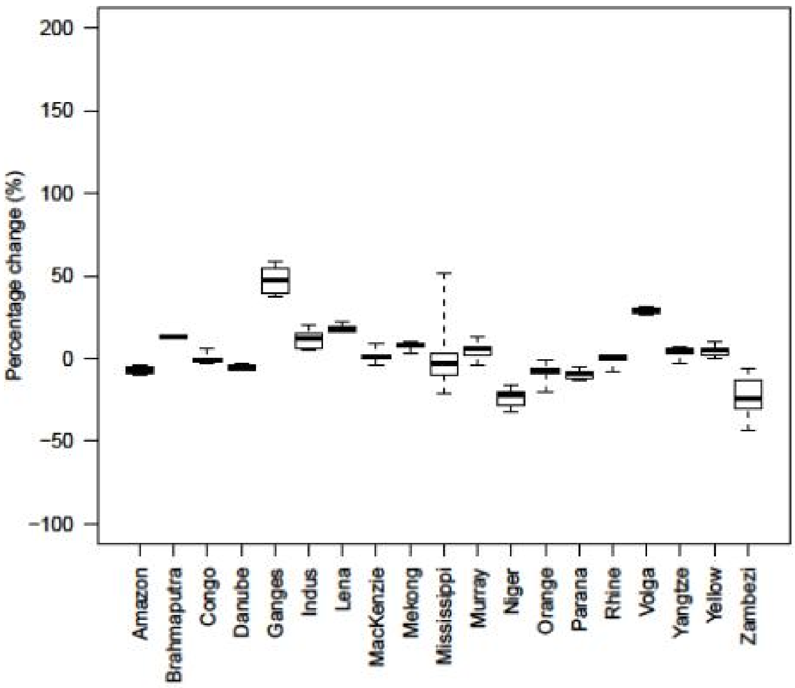


**a.**

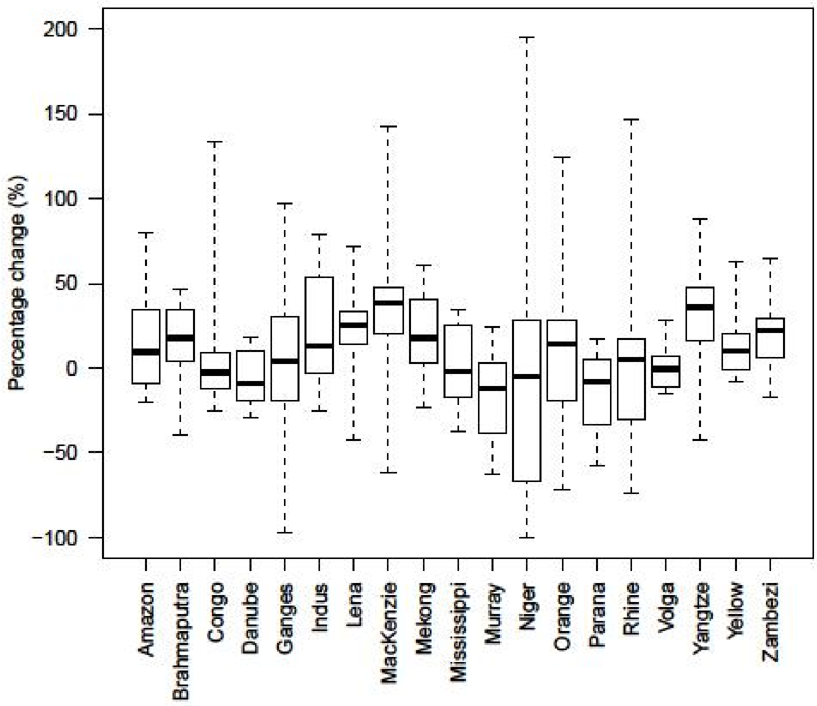


**b.**

Figure 13a. Boxplots of changes projected by the five available realizations of the GCM CGCM 2.3.2 for the A1B scenario for 2100. Whiskers mark the maximum and minimum projected changes, boxes span the quartile range and horizontal dashes represent the median of projected changes. Figure 13b. same as Fig. 13a. but now for the changes projected by the ensemble of 12 GCMs.

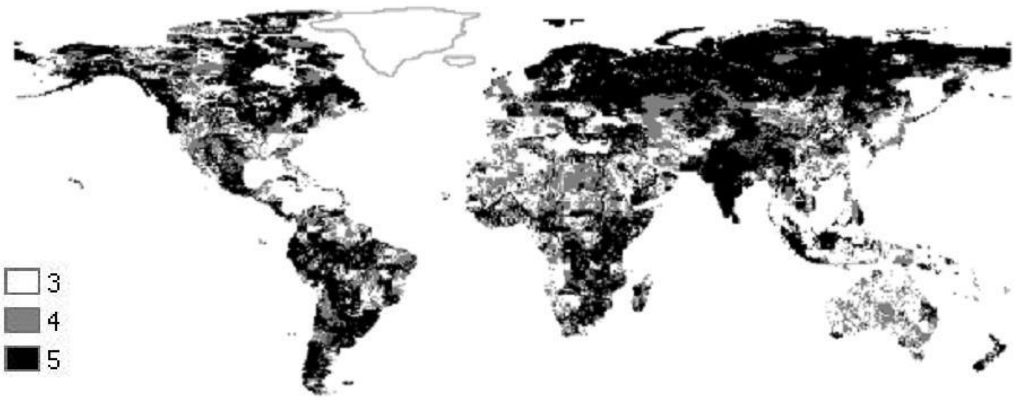


Figure 14: Map showing the number of realizations of CGCM2.3.2 projecting mean change in the dominant direction. Black indicates regions where the five realizations project changes in the same direction, grey indicates regions where four realizations project similar directions of change and in the white regions only three realizations project the same direction of change. The dominant direction is the direction of change projected by the majority of models.